ELSEVIER

Earth and Planetary Science Letters 138 (1996) 93-104

EPSL

Hydrothermal exploration near the Azores Triple Junction: tectonic control of venting at slow-spreading ridges?

C.R. German *, L.M. Parson, HEAT Scientific Team [1]

Southampton Oceanography Centre, Empress Dock, Southampton, SO14 3ZH, UK

Received 8 June 1995; accepted 14 November 1995

Abstract

Simultaneous acoustic imaging of the seafloor and detection of particle-rich plumes in the overlying water column have been used to identify and determine the tectonic setting of high-temperature 'black smoker' hydrothermal activity along 200 km of the Mid-Atlantic Ridge between 36° and 38°N. Using this approach, we have identified hydrothermal signals at 7 different locations. These results indicate a higher incidence of hydrothermal activity along this section of ridge axis than has been reported elsewhere along slow spreading ridges.

Our data show that the majority of hydrothermal sites here are located near to non-transform offsets rather than at the centres of individual ridge segments. We suggest that this intersection of fabrics, associated with ridge discontinuities and the spreading process, is instrumental in focussing hydrothermal flow at these localities. Future strategies of exploration for hydrothermal activity on slow-spreading ridges may need to be revised accordingly.

Keywords: Azores; Mid-Atlantic Ridge; triple junctions; black smokers; acoustical surveys

1. Introduction

Neutrally buoyant plumes overlying high-temperature 'black smoker' hydrothermal fields exhibit pronounced enrichments compared to ambient seawater in a range of characteristic tracers. Consequently, analysis of water-column samples can be a powerful tool for prospecting for the presence of hydrothermal activity in previously unexplored sections of mid-ocean ridge crest (e.g. [1] and refs. therein). Key dissolved tracers which have been used for this in the past include ^3He, Mn, CH_4 and — to a lesser extent — ^{222}Rn and H_2 (e.g. [2–5]). A limitation of these approaches is that they have typically relied upon collection of discrete samples for shore-based or ship-board analysis, yielding only limited data

* Corresponding author. Fax: +44 1703 596554. E-mail: C.R.German@soc.soton.ac.uk

[1] HEAT Scientific Team: C.R. German [1], L.M. Parson [1], H. Bougault [2], D. Coller [3], M. Critchley [3], A. Dapoigny [4], C. Day [1], D. Eardley [5], A. Fearn [1], C. Flewellen [1], R. Kirk [1], G. Klinkhammer [6], J.-Y. Landuré [2], E. Ludford [7], M. Miranda [8], H.D. Needham [2], J. Patching [5], R. Pearce [1], H. Pellé [2], J. Radford-Knoery [2], I. Rouse [1], J. Scott [1], P. Stoffregen [6], P. Taylor [1], D. Teare [1] and J. Wynar [1]. ([1] Southampton Oceanography Centre, Southampton, UK; [2] IFREMER Centre de Brest, France; [3] ERA-MAPTEC, Dublin, Ireland; [4] CEA-Saclay, France; [5] Department of Microbiology, University College Galway, Ireland; [6] COAS, Oregon State University, USA; [7] Department of Geology, University of Bristol, UK; [8] Department of Geophysics, University of Lisbon, Portugal.)

SSDI 0012-821X(95)00224-3

coverage. More recently, optical sensors — both nephelometers, which record light scattering, and transmissometers, which record light attenuation — have been widely used to prospect for and investigate hydrothermal plumes along various sections of the global mid-ocean ridge system (reviewed in [1]).

In this study we describe the results from an investigation into the occurrence of hydrothermal plumes overlying a section of the slow-spreading Mid-Atlantic Ridge (36–38°N), close to the Azores Triple Junction. The objective of the project was to identify new sites of hydrothermal activity along the ridge-crest, as well as simultaneously acquiring detailed acoustic imagery of the seabed in the areas of venting. Our goal, in combining these approaches, was to determine geological constraints upon the occurrence of hydrothermal activity on the Mid-Atlantic Ridge and, thus, derive the basis for a predictive model for the location of hydrothermal activity on other slow-spreading ridge systems.

2. Methodology

All work described in this paper was carried out as part of RRS *Charles Darwin* cruise CD89/94 [6]. The instrument used for this study was TOBI (Towed Ocean Bottom Instrument), SOC's deep towed sidescan sonar platform. As well as the principal 30 kHz sidescan sonar, the vehicle was equipped with a 7.5 kHz seismic profiler, a tri-axial fluxgate magnetometer, a thermistor temperature sensor and a SeaTech 25 cm transmissometer (cf. [7]). The instrument was towed astern of the ship at speeds of ~ 1.5 knots and at altitudes of 150–500 m above the seabed. In this manner over 200 km of transmissometer data,

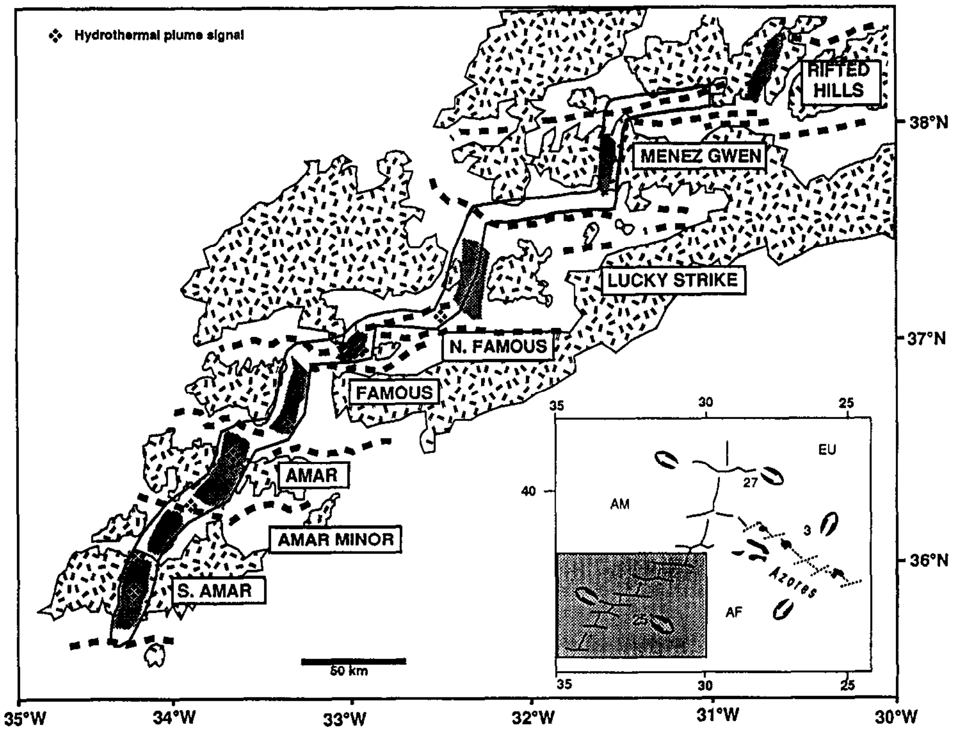

Fig. 1. Tectonic setting of the study area, MAR 36–38°N, illustrating the distribution of right-stepping second-order segments (axial zones in dark stipple) and their bounding non-transform discontinuities (solid dashed lines). Shading with random dashes indicates seafloor shallower than 1500 m. Active non-transform discontinuity (NTD) sections are locally complex and multiple off-axis traces suggest temporal instability of segment lengths. Heavy lines outlining the ridge-axis and offsets, 36–38°N, indicate the full extent of TOBI sidescan insonification. Inset locates this ridge section (stippled box) within the larger Azores Triple Junction area. *AM* = American plate; *EU* = Eurasian plate; *AF* = African plate. Arrows indicate 100° plate motion direction at 25 mm/yr full spreading rate.

co-registered with 1500 km^2 of TOBI sidescan sonar imagery of the seabed, were collected between 36°N and 38°N along the axial valley and right-lateral non-transform discontinuities which offset the Mid-Atlantic Ridge. Follow-up vertical profiling was performed using a Neil Brown MkIII CTD-rosette equipped with a Chelsea Aquatracka MkII Nephelometer.

3. Results

The regional pattern of ridge geometry between 36° and 38°N has been outlined by Needham et al. [8] and Detrick et al. [9] following a systematic programme of detailed swath multibeam bathymetric surveying. Seven second-order ridge segments, ranging from 20 to 55 km in length, are separated by six, right-stepping non-transform discontinuities, resulting in an overall ridge azimuth of 045° (Fig. 1). The principal extension direction is 100°, and a present-day estimated full spreading rate of 25 mm/yr has been determined by Sloan and Patriat [10].

Our TOBI sidescan sonar data were recorded during single and locally double survey swaths throughout the axial floor of each of these segments and, thus, provide between 6 and 12 km swath insonification (Fig. 1). These images are crucial for the determination of both the extent of the neovolcanic activity and the varying degree of deformation along and across the axial zone. Continuous data were also acquired along the ridge offsets, which in most examples between 36° and 38°N tend to be represented by broad open valleys, up to 25 km wide with irregularly disposed walls, and follow only a loose approximation to the plate motion (Fig. 1). The detailed analysis of these features is beyond the scope of this paper, but it is relevant to note that the sedimented floors of the discontinuities are frequently cut by arrays of en echelon and locally conjugate fault structures. There is no evidence for neovolcanic activity, although a number of highly deformed volcanic blocks can be observed stranded within or straddling several of the offsets.

During at-sea operations the smallest transmissometer anomalies which could readily be discerned from the on-stream data sets were those with a greater than 0.025% decrease in percentage transmission from background anomalies. Discernable transmissometer anomalies, according to this definition,

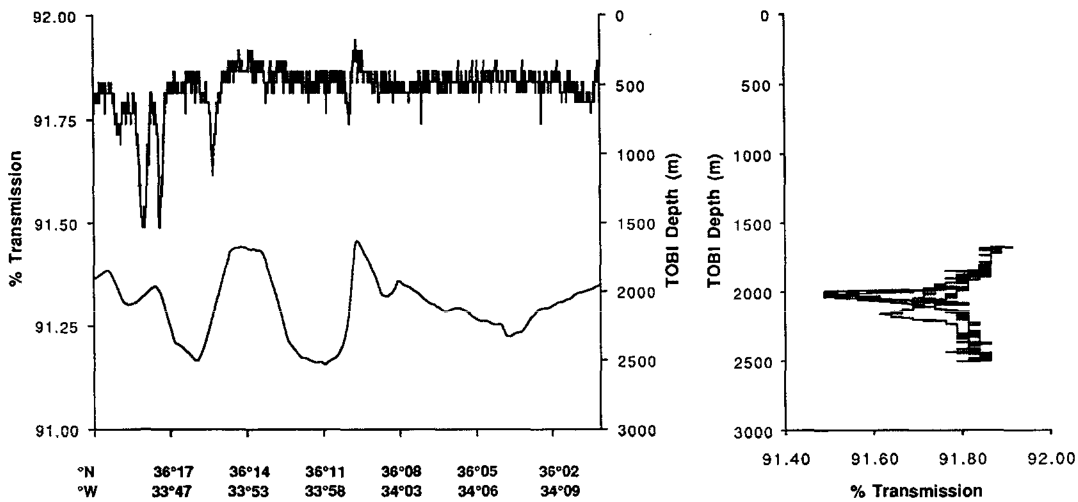

Fig. 2. Left: Profiles of transmissometer data (upper) and instrument depth (lower) as recorded from TOBI during an along-axis tow through the AMAR–AMAR Minor offset between 36°20′N and 36°00′N, MAR. Note pronounced drops in transmissometer signal at 36°18′N and 36°17′N and less pronounced, but still significant, transmissometer anomalies at 36°19′N, 36°15′N and 36°10′N. Right: TOBI transmissometer data between 36°20′N And 36°10′N replotted against TOBI depth. Note that all five plume anomalies seen in the left-hand figure now reduce to a common, coherent hydrothermal plume centred at 2000–2200 m depth, which is absent from the water column at the same depths between 36°10′–36°00′N.

were recorded along 14 different sections of TOBI track during the survey. However, because double passes of TOBI were made through many sections of the survey area, we can only assign these 14 signals to 7 broad geographic locations at which particle-rich hydrothermal plume signals were observed (Fig. 1). The maximum transmissometer anomalies recorded at each location are presented, along with the full extent of the TOBI tracks along which those anomalies were recorded, in Table 1. Transmissometer data can be presented both in terms of the percentage of light transmission (T) or as beam attenuation, c, where $c = -\ln(T)/r$ (r = transmissometer path length, 25 cm in this study). At-sea data is detected as percentage transmission (T), whilst the recalculated beam attenuation (c) has previously been shown

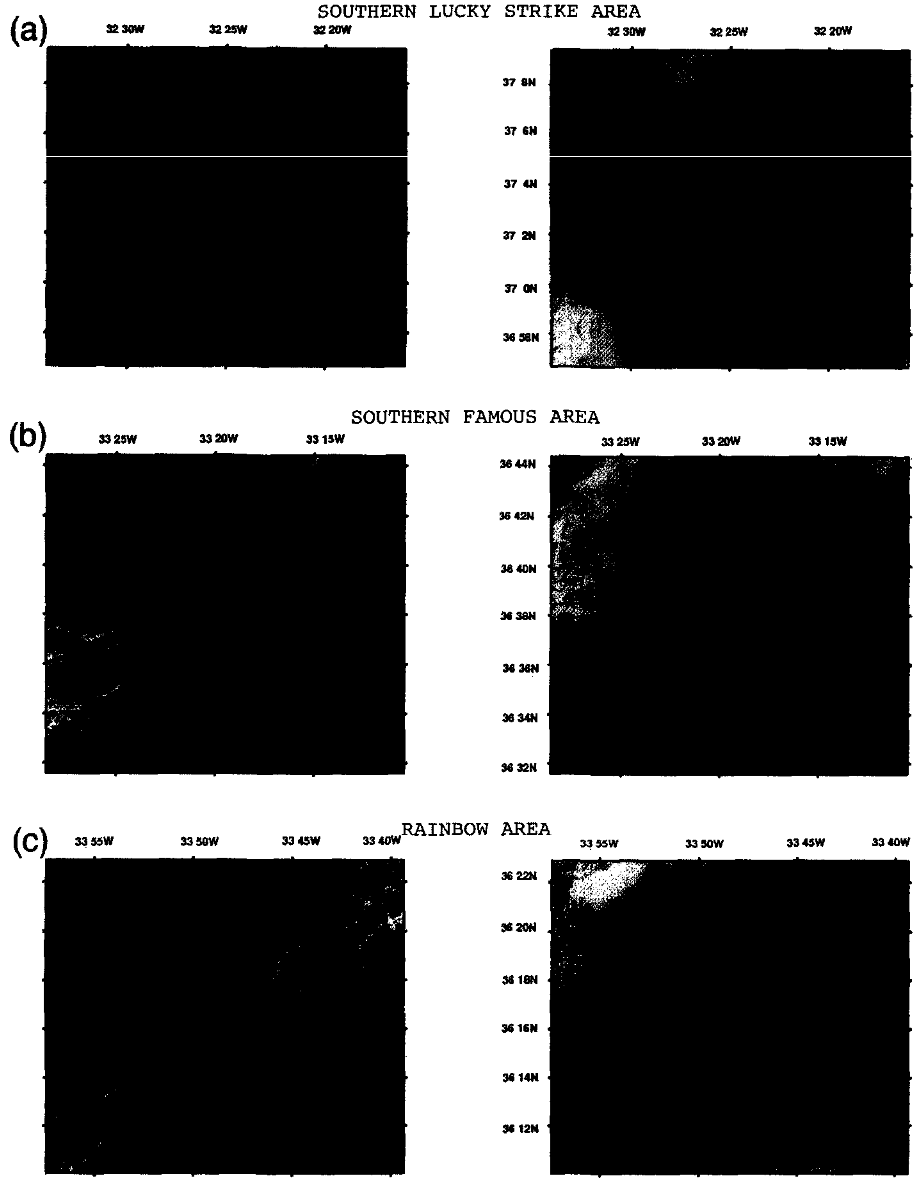

to exhibit a linear correlation with particle mass concentration [1]. To allow direct comparison with previous TOBI transmissometer data from Broken Spur [7], our data is presented graphically, below, as the percentage transmission (T) but data values for transmissometer anomalies in Table 1 are also listed as both ΔT and Δc to aid comparison with other studies from (e.g.) the East Pacific Rise and Juan de Fuca Ridge [1]. The largest anomaly detected (approximately double that observed during the comparable survey which discovered the 1993 Broken Spur site, [7]) was located close to 36°18′N (Fig. 2a) in the offset between the AMAR (Alvin Mid Atlantic Ridge) and AMAR Minor segments — the Rainbow hydrothermal area. Because it is known that hydrothermal plumes over the Mid-Atlantic Ridge can

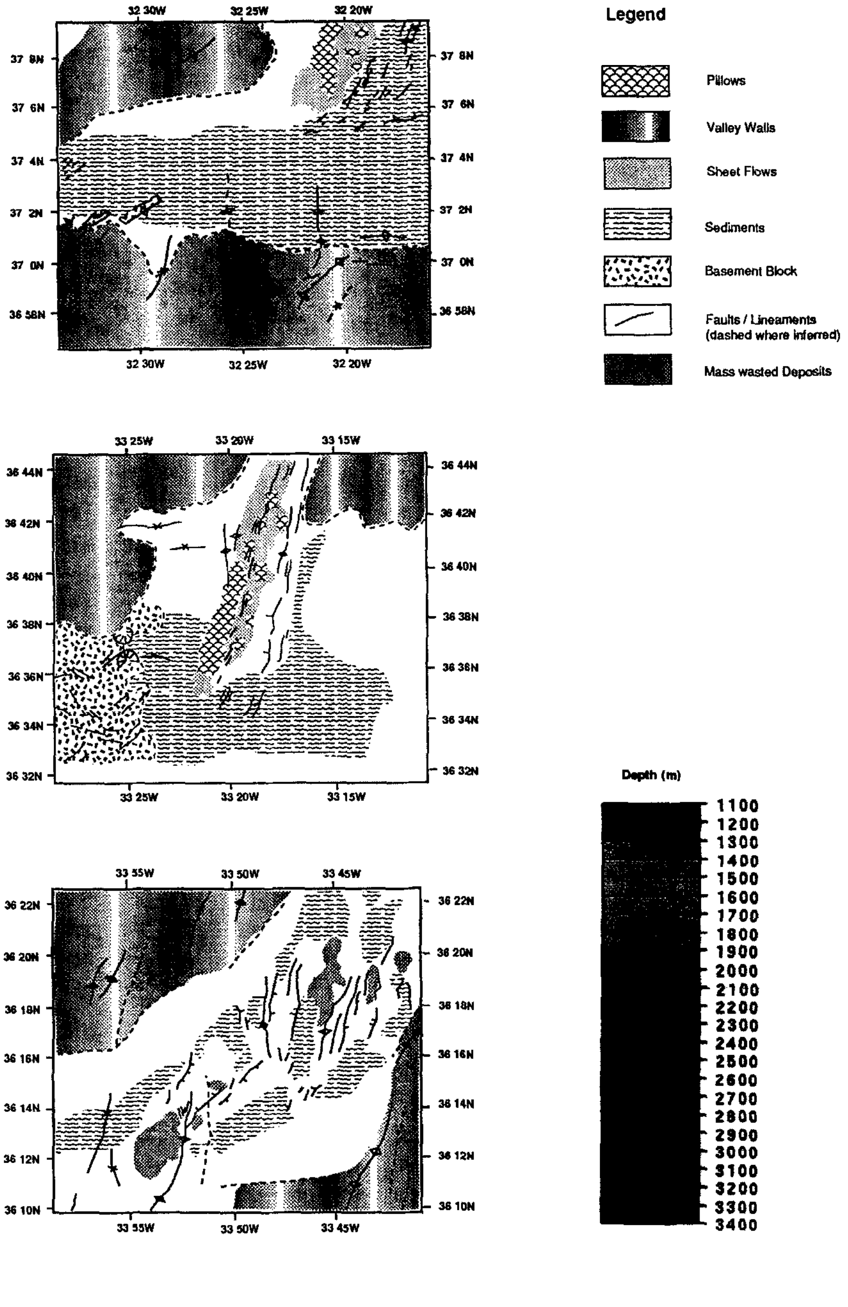

Table 1
Hydrothermal plumes on the Mid-Atlantic Ridge, 36–38°N

No.	Segment	Anomaly Size (% T)	Anomaly Size (c)	Location
#1	Sth. Lucky Strike	0.05	-0.0022	37°03'N 32°31'W - 37°03'N 32°36'W
#2	North FAMOUS	0.05	-0.0022	36°59'N 32°57'W - 36°57'N 33°00'W
#3	FAMOUS	0.10	-0.0044	36°38'N 33°19'W - 36°34'N 33°21'W
#4	AMAR	0.15	-0.0065	36°29'N 33°41'W - 36°25'N 33°42'W
#5	AMAR/AMAR Minor	0.38	-0.0163	36°18'N 33°45'W - 36°14'N 33°53'W
#6	South AMAR	0.05	-0.0022	36°05'N 34°04'W - 36°04'N 34°05'W
#7	South AMAR	0.03	-0.0011	36°00'N 34°11'W - 35°57'N 34°12'W

Results from TOBI transmissometer data: CD89/94.

extend for several kilometres through the water column away from their individual sources [3,20], it is to be expected that multiple anomalies in close proximity should not necessarily indicate interception of multiple discrete plumes but, instead, could indicate repeat crossings by the instrument of the same hydrothermal plume. A clear example of this is shown in Fig. 2b where the combined percentage transmission data for the TOBI track between 36°20′N and 36°09′N, when replotted against instrument depth, collapses from a series of 5 discrete percentage transmission anomalies, located at 36°19′N, 36°18′N, 36°17′N, 36°15′N and 36°10′N, into a single coherent plume, centred at 2000–2200 m depth, which extends throughout this section of the MAR rift valley. Further large anomalies were also observed further north in the AMAR segment, close to previously recorded nephelometer and transmissometer profile anomalies [11] and in the FAMOUS (French American Mid Ocean Underwater Study) segment (Fig. 1), where deep-water anomalies in dissolved CH_4 had previously been identified [12].

At the southern end of the Lucky Strike segment transmissometer anomalies were identified above the sediment-mantled portion of the offset at 37°03′N 32°31–36′W (Table 1, plume #1; Fig. 3a). These signals were subsequently confirmed during a CTD–nephelometer–transmissometer station, which indicated a small but distinct nephelometer anomaly at 1750–1800 m depth within this sub-basin (Fig. 4, left). The size of the anomaly is comparable with those reported from directly above the previously identified Lucky Strike vent field at 37°15′N [11,13], as were particulate Fe concentrations measured in filtered seawater samples from this location (E. Ludford, pers. commun., 1995). However, because they are located in the non-transform offset south of the segment containing the Lucky Strike site [14,15], the signals reported here most certainly derive from an additional, quite discrete source of hydrothermal venting. Apart from a single, north-facing fault cutting the sedimented southern termination of the Lucky

Fig. 3. aTOBI deeptow sidescan sonographs, swath bathymetry (centre) and line-drawn geological interpretations of: above: eastern section of NTD between North FAMOUS and Lucky Strike segments; centre: eastern section of NTD between FAMOUS and AMAR; below: a section of the AMAR/AMAR Minor offset. Lighter tones in sidescan sonographs (left) are areas of greater reflectivity. The locations of the TOBI sidescan sonar data are outlined on the bathymetric maps (centre) in red. Isobath intervals are 50 m (data from [8]) with colour change intervals every 100 m. Above: The irregular mottled texture in the northeast of the TOBI sonograph at southern Lucky Strike corresponds to mounded pillow constructions forming the southern limit of an axial volcanic ridge. This mounded topography is surrounded by bright, flat-lying lava sheet extrusives which overly weakly back-scattering (darker) uniform-textured sediments. Oblique, faulted ridges in the west of the image have bright flanks, interpreted as talus associated with active faulting and weathering. The transmissometer anomaly detected along the TOBI track is highlighted in yellow, and the location of follow-up station CTD 08 (Fig. 4, left) is marked by the yellow dot. Centre: The intensely lineated, brightly backscattering eastern portion of the TOBI sonograph in the southern FAMOUS area corresponds to the pervasively faulted and fissured neovolcanic floor of the FAMOUS segment. Few areas of unfaulted, mounded axial volcanic ridges are recognised. Uniformly backscattering sedimented pockets separate the segment end from a highly reflective mottled zone in the west of the image. This latter area corresponds to a deformed and weathered block extending from the west flank of FAMOUS into the NTD. The transmissometer anomaly detected along the TOBI track is highlighted in magenta, and the location of follow-up station CTD 02 (Fig. 4, centre) is marked by the magenta dot. Below: The fault-dominated NTD zone in the Rainbow (AMAR/AMAR Minor offset) area is characterised by a series of well spaced major north–south and northeast–southwest structures which separate areas of sedimented seafloor which is, itself, intensely faulted locally. Transmissometer anomalies were detected along-track (highlighted in red) between two relict blocks within the NTD (Rainbow Ridge is the more southwesterly of the two) which show extensive faulting and mass wasting deposits. The location of follow-up station CTD 10 (Fig. 4, right) is marked by the red dot.

Strike segment (Fig. 3b) there are no clear spreading-parallel fabrics cutting the southern sub-basin overlying the ridge-offset intersection. However, obliquely trending ridges associated with extensional horst and graben formation are observed further west within the left-lateral offset. These are inferred to be currently active because of the occurrence of adjacent talus aprons which have not yet been buried by more recent sedimentation (Fig. 3). The nearest neovolcanic activity observed in the TOBI images occurs in the form of lava sheets and axial volcanic ridge constructs, which are observed some 15 km northeast of the location of the hydrothermal plume anomalies, adjacent to the west wall of the southern end of the Lucky Strike segment, sensu stricto.

A more significant transmissometer anomaly was recorded from TOBI at the southern limit of the FAMOUS segment between 36°38′N 33°19′W and 36°34′N, 33°21′W (Table 1, plume #3; Fig. 3). Although a subsequent CTD–nephelometer–transmissometer profile revealed only a very weak nephelometer signal at this location (Fig. 4, centre) this may, in part, be due to clouding of the nephelometer window for this deployment (note high mid-water background voltage in Fig. 4 CTD 02 compared to CTD 08 (southern Lucky Strike) and CTD 10 (Rainbow)). Nevertheless, the plume anomaly centred at 2250–2300 m water depth, coincides closely with the depth of dissolved CH_4 anomalies reported previously from the southern section of this segment [12] and also coincides with anomalously high dissolved Mn concentrations recorded using the Oregon State University ZAPS in situ dissolved Mn sensor (G. Klinkhammer, pers. commun., 1995). Above-background North Atlantic particulate Fe concentrations (~ 10 nmol/l) were also recorded at this location (E. Ludford, pers. commun., 1995), further confirming the high-temperature characteristics of the underlying vent source. Again, these signals were recorded from a non-volcanic section of the segment — one which is characterised by a complex series of cross-cutting fault fabrics both parallel to and sub-orthogonal to the extensional direction (Fig. 3, centre).

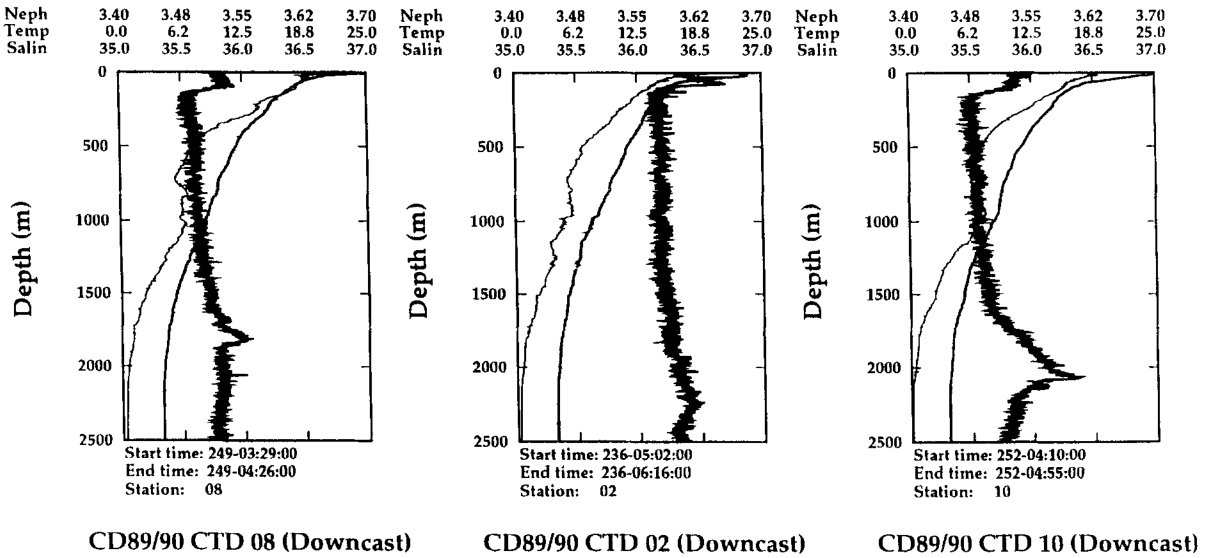

Fig. 4. Vertical profiles of salinity (thinnest line), temperature and nephelometer (heaviest line) data recorded from vertical profiles in the southern Lucky Strike area (CTD 08), the southern FAMOUS segment (CTD 02)and the Rainbow area (AMAR/AMAR Minor offset; CTD10). Note the particle-rich nephelometer signal, 1750–1800 m, at station CTD 08 (southern Lucky Strike); the weak particle-rich nephelometer signal, 2250–2300 m, at station CTD 02 (FAMOUS) and the strong particle-rich nephelometer signal, 1700–2150 m, at station CTD 10 (Rainbow). Note also the increased background nephelometer reading (~ 3.55) at FAMOUS, due to initial clouding of the nephelometer during this early cast (CTD 02), which may have obscured the true magnitude of the anomaly at this site when compared to the subsequent deployments at Lucky Strike and Rainbow (CTDs 08 and 10; nephelometer background ~ 3.48).

More regional bathymetric compilations confirm persistent transverse (spreading-parallel) structures outside of the discontinuity trace [9].

Within the non-transform discontinuity (NTD) between the AMAR and AMAR Minor segments (the Rainbow area), pronounced transmissometer anomalies were recorded between 36°18′N,33°45′W and 36°14′N,33°53′W (Table 1, plume #5; Fig. 3, below). Clear hydrothermal plume signals were observed throughout the water column at this location, centred at 2000–2200 m (Fig. 2, right and Fig. 4, right), with anomalies recorded from the vertical CTD–nephelometer profile being comparable in magnitude to those reported previously from the TAG hydrothermal field, 26°N, Mid-Atlantic Ridge (e.g. [16,17]). This data has been further confirmed by particulate Fe concentrations from the same location as the CTD profile shown in Fig. 4 (right), which approach 100 nmol/l (E. Ludford, pers. commun., 1995), indicating, once more, that these plume signals are a direct result of high-temperature hydrothermal venting from the seabed. The seafloor in this area is characterised by sedimented sub-basins and pervasively faulted, stranded volcanic blocks (Fig. 3, below). Fault families include inward facing normal offsets of up to 500 m, which define an en echelon array of rift valley wall sections and subtend outlying volcanic ridges. These latter features may be spalled portions of the valley walls or reflect ephemeral phases of increased magmatic productivity. The most numerous structures are tightly spaced, small-amplitude faults, with a throw of less than 50 m, which occur both parallel to segments and obliquely across the discontinuity basin. The Rainbow Ridge, at 36°12–15′N,33°53′W, is dissected by several sets of faults; sidescan records show a wide range of erosional and mass-wasting textures, suggesting that degradation is well advanced.

A feature common to five of the seven hydrothermal plume signals reported here (Plumes 1–3, 5 and 6; Table 1) is that they are not located towards the centres of ridge segments but, instead, occur within or adjacent to the non-transform discontinuities which offset the segments. We expand on these observations, below, in order to determine whether the high frequency of hydrothermal activity reported here is related to the increased thermal effect of the Azores hot spot, to our more systematic sampling techniques, or to some tectonic control from intersecting fault fabrics.

4. Discussion

Due to the fact that the TOBI instrument is towed at almost constant height, sub-parallel to the seabed, rather than being 'tow-yoed' through the water column like a CTD package (e.g. [1,18]), the transmissometer data collected from TOBI during CD89 may not have intercepted every particle-rich hydrothermal plume present in the MAR rift valley, 36–38°N. Indeed, we are aware of at least two occasions in which our survey definitely *failed* to intercept a known neutrally buoyant plume signal because the instrument was towed either too high or too low (see below). Nevertheless, our survey has revealed evidence for at least 7 discrete sources of hydrothermal activity over just 200 km of ridge crest, representing a minimum average frequency of one vent site every 25–30 km. This represents a much higher frequency than that determined from previous studies of the Mid-Atlantic Ridge, where average plume occurrences were approximately one every 150–175 km (e.g. [1,19]). Below we examine possible influences which might give rise to this greater apparent incidence of venting along the MAR, 36–38°N.

4.1. Increased heat flow from the Azores hot spot?

In general, the influence of hot spots on mid-ocean ridge processes and, in particular, the effect upon segmentation character and magmatic supply, is poorly understood. The Azores hot spot, believed to lie to the east of the plate triple junction, is less well documented than most. Certainly, the regional scale bathymetry of the region 38–40°N shows an anomalously elevated topography, reflecting unusually high melt generation and, thus, crustal thickening at this section of the Mid-Atlantic Ridge [8]. A typical slow-spreading ridge rift valley is largely absent from the 38–40°N section of the ridge crest but, south of 38°N, the rift valley becomes rapidly and progressively better developed towards 36°N, the southern limit of this study. This phenomenon, together with observations from gravity studies, has led Detrick et al. [9] to conclude that hot spot influence is largely absent from the ridge crest south of 38°N. In combination with our earlier work, which showed a surprisingly low incidence of hydrothermal activity along the Reykjanes Ridge close to the Iceland hot spot [20], this leads us to conclude that the Azores hot spot has little influence upon the incidence of venting along the Mid-Atlantic Ridge between 36° and 38°N.

4.2. Horizontal sampling versus vertical profiling

The present study used a transmissometer, towed along-axis, mounted upon our deep-towed instrument TOBI. This is an unusual departure from most previous studies on the Mid-Atlantic Ridge which, primarily, have focused upon vertical profiling at the centres of discrete segments. We recognise, therefore, that the increased incidence in hydrothermal venting reported in this paper may simply reflect the fact that continuous surveying has increased the total length of ridge crest which has been investigated and sampled when compared to previous work. Whilst this comparison remains valid for the majority of previous studies along the Mid-Atlantic Ridge (e.g. [3,4,11,12,17]) an important exception is the work by Murton et al. [7], which involved the discovery of the Broken Spur vent site. During that work, an identical survey technique was used, completing a double-swath TOBI transmissometer survey of the entire Mid-Atlantic Ridge crest between 27°N and 30°N. However, evidence for hydrothermal activity was only reported at three discrete locations from that work, at an average spacing of one site per 100 km (cf. one site per 25–30 km, 36–38°N). Clearly, therefore, the increase in incidence of vent activity observed during our study cannot be attributed to the novel TOBI surveying strategy alone.

4.3. Neovolcanic versus tectonic control?

An important difference between the 36–38°N and 27–30°N study areas is the increased degree of segmentation in the more northern study. The average spacing of segments between 27°N and 30°N is approximately 52 km, compared to less than 39 km for that of the MAR south of the Azores. A higher frequency of discontinuities is compounded by our observations that the offset zones between 36° and 38°N are broad, up to 20 km in width, and characterised by complex patterns of oblique and parallel faulting. These faults locally extend into the segment ends where significant transverse (i.e. extension-parallel) structures interrupt both axial valley walls and axial floor morphology. These observations lend support to scientific arguments that tectonic control may play an important part in determining the setting of hydrothermal activity. This is not to preclude the possibility that areas of fresh neovolcanic activity can also host hydrothermal activity. Previous work at MAR segment centres has led to the discovery of hydrothermal activity which is associated with recent, neo-volcanic activity (e.g. Snakepit, 23°N [21]; Broken Spur, 29°N [7]; Lucky Strike, 37°N [14,15]; Menez Gwen, 38°N [15] and Steinahóll, 63°N [20]). Similarly, high-temperature hydrothermal activity on the fast-spreading East Pacific Rise is typically restricted to the neovolcanic ridge axis too, occurring almost exclusively within the axial summit caldera (e.g. [22–24]). It is interesting to note, however, that even at the recent eruptive sites discovered on the fast-spreading EPR (9–11°N), detailed investigations are increasingly leading to the conclusion that crustal fissuring plays an important role in constraining the presence and manifestation of seafloor hydrothermal venting [25].

Five of the seven new locations at which hydrothermal signals have been identified during this study are characterised by highly tectonised oceanic crust, with or without sediment accumulation, but with the absence of any fresh neovolcanic eruptive and/or constructional features. Our TOBI data indicate that axis-parallel faults, with throws of between 5 m and 300 m, intersect with two subordinate populations of structures, one of which is oriented parallel to the NTDs, whilst the other exhibits oblique northeast–southwest trends (Fig. 3 and L.M. Parson, unpubl. data). Oblique faulting is particularly prevalent in the broad NTD zones, where, locally, deformation appears to pervade their entire width. Fabrics associated with ridge offset/segmentation are not confined to these broad NTD zones, however. The bathymetry data show that outside of the offsets, deep linear embayments parallel to the NTDs cut into both segment walls (e.g., FAMOUS segment, Fig. 3, 36°41′N,33°20′W to 36°42′N,33°25′W) and

NTD walls (e.g., west of Rifted Hills segment, Fig. 1, 38°09′N,31°00′W).

The tectonism of this section of ridge, both inter- and intra-segment, is extensive and pervasive. Our sidescan data have been used to demonstrate complex intersecting fabrics in the near-NTD areas where hydrothermal activity appears to be preferentially located and, conversely, to confirm local neovolcanic activity at the centres of segments, where significantly fewer hydrothermal signatures were recorded. Consequently, we conclude that crustal fissuring must be of importance in controlling the incidence of hydrothermal activity along slow-spreading ridge sections such as the Mid-Atlantic Ridge. Furthermore, we note that our mapping of intersecting transverse fabrics supports our suggestion that this relationship is likely to contribute to the focussing of fluid flow and the localisation of vent sites.

4.4. Limitations of TOBI transmissometer surveys

It is of interest to note that no TOBI transmissometer anomalies were detected immediately above either the Menez Gwen or the Lucky Strike hydrothermal fields (37°50′N and 37°15′N), despite TOBI having been surveyed through these areas at just 300–500 m off bottom (Fig. 1). In Menez Gwen, this is readily explained because the erupting fluids are almost entirely phase-separated and, thus, are volatile-rich but essentially metal-free [15]. Consequently, any resultant neutrally buoyant plume exhibits no anomalous Fe/Mn oxyhydroxide particulate enrichments and no transmissometer anomaly would be expected. The Lucky Strike vent fluids are also anomalously metal-poor when compared to more conventional black smokers for which the overlying plume signals for (e.g.) transmissometer anomalies are already well known to be difficult to detect [13]. Data transmission problems during our first TOBI tow-track from north to south through the central Lucky Strike segment further hindered our initial work because no discernable anomalies were resolved at depths of approximately 1400 m during our first pass through this area. This problem was resolved in time for the commencement of our second tow, which continued south from the southern end of the Lucky Strike segment (Figs. 1 and 3, upper) and did not recur throughout the remainder of the expedition. However, upon our return north through the central Lucky Strike segment, a key objective was to obtain optimal sidescan sonar images of the lava lake known to characterise the seafloor at the centre of the axial volcanic complex which hosts the hydrothermal activity. Because of the steep-sided nature of the local terrain, optimised imaging (with minimal shadowing) could only be obtained by flying TOBI high above the complex, at a water depth close to 1000 m; that is, significantly shallower than the depths at which hydrothermal plume anomalies had previously been identified (1200–1750 m, [13]). Again, no transmissometer anomalies characteristic of hydrothermal plume signals were detected. This re-affirms the two principal limitations of a TOBI transmissometer survey strategy: (1) transmissometer anomalies will only be detected where water depths are sufficient for conventional particle-rich (non phase-separated) hydrothermal plumes to be generated; (2) the overriding importance of TOBI as a seafloor imaging instrument dictates that the instrument may often be flown at an altitude above the seafloor which does not coincide with the depth at which neutrally buoyant plumes occur. We have observed a second example of the latter in the case of the southern AMAR segment, in which a northward tow through the area, following the crest of a neo-volcanic ridge, indicated the presence of a hydrothermal plume at 36°04–05′N at depths between approximately 1600 m and 1800 m (Table 1, plume #6). Re-examination of the first flight of our TOBI transmissometer system through this segment revealed that no such signals had been intercepted previously, because TOBI had been following the deeper western portion of the rift valley floor and, consequently, flying *beneath* the depth of the neutrally buoyant plume (Fig. 2, left).

5. Summary and conclusions

Deep-tow detection of particle-rich hydrothermal plumes was carried out in conjunction with seafloor sidescan sonar imaging of the Mid-Atlantic Ridge between 36° and 38°N, using a combination of a 25 cm path-length transmissometer mounted on the SOC's Towed Ocean Bottom Instrument (TOBI). Our survey has revealed evidence for seven discrete sources of hydrothermal venting, representing an average frequency of occurrence of approximately one vent site every 25–30 km. This represents a minimum five-fold increase in the apparent frequency of occurrence of hydrothermal vent sites along the MAR compared to previous studies. Further, of the seven discrete sites at which evidence for venting was observed, at least five sites occur at or close to the ends of second-order ridge discontinuities. Each of these five locations is characterised by highly tectonised oceanic crust, with or without sediment accumulation, but in the absence of any fresh neovolcanic eruptive and/or constructional features. Two families of cross-cutting fault fabrics typically characterise these regions.

From these observations we are able to draw the following conclusions:

1. Tectonic parameters appear to be the dominant controlling force on the location of focused hydrothermal activity on a 200 km section of the slow-spreading Mid-Atlantic Ridge near the Azores Triple Junction, 36–38°N.
2. Within the present study, sites of hydrothermal activity have been found to be more common towards the ends of second-order segments, or within the offset zones linking these segments. We suggest that this increase in occurrence is in direct proportion to the local cross-cutting fault fabrics at segment termini.
3. Traditional exploration strategies, using vertical profiling to target the central portions of segments alone, are of limited applicability for fast- and slow-spreading ridges alike. Such strategies have long been recognised as being inadequate at fast-spreading ridges, where magma delivery tends towards a two-dimensional distribution. This work shows that the same approach is also likely to underestimate significantly the incidence of hydrothermal activity at slow-spreading ridges, where venting may previously have been considered to be dominated by simple melt delivery to segment centres.

Acknowledgements

We thank Capt. R.A. Bourne, the officers and crew of RRS *Charles Darwin* for their skill, professionalism and enthusiasm throughout HEAT cruise CD89/94. We also thank Rachel Cave and Richard Miller (IOSDL) for their assistance in data processing and figure drafting for this manuscript. RRS *Charles Darwin* cruise CD89 (HEAT) and follow-up work at SOC (formerly IOSDL) was jointly funded by the UK Community Research Programme 'BRIDGE' and by EC Marine Science and Technology contract MAST-MAS2 CT93-0070 'MARFLUX/ATJ', coordinated by Dr. H. Bougault at IFREMER Centre de Brest, France. The manuscript has benefitted significantly from the careful and considered reviews of Dr. Ed Baker, Dr. Susan Humphris and Dr. J.-C. Semperé. SOC/IOSDL contribution no. 95032. *[CL]*

References

[1] E.T. Baker, C.R. German and H. Elderfield, Hydrothermal plumes: global distributions and geological inferences, in: Seafloor Hydrothermal Systems: Physical, Chemical, Biological and Geological Interactions, S.E. Humphris et al., eds., Geophys. Monogr. 91, 47–71, 1995.

[2] J.E. Lupton and H. Craig, A major helium-3 source at 15°S on the East Pacific Rise, Science 214, 13–18, 1981.

[3] G. Klinkhammer, P. Rona, M.J. Greaves and H. Elderfield, Hydrothermal manganese plumes over the Mid-Atlantic Ridge rift-valley, Nature 314, 727–731, 1985.

[4] J.L. Charlou, P. Rona and H. Bougault, Methane anomalies over TAG hydrothermal field on Mid-Atlantic Ridge, J. Mar. Res. 45, 461–472, 1987.

[5] D.C. Kadko, N.D. Rosenburg, J.E. Lupton, R.W. Collier and M.D. Lilley, Chemical reaction rates and entrainment within the Endeavour Ridge hydrothermal plume, Earth Planet. Sci. Lett. 99, 315–335, 1990.

[6] C.R. German, et al., Hydrothermal Exploration at the Azores Triple Junction. RRS *Charles Darwin* Cruise CD89/94. IOS Deacon Laboratory Cruise Rep. 246, 58 pp., 1995.

[7] B.J. Murton, G. Klinkhammer, K. Becker, A. Briais, D. Edge, N. Hayward, N. Millard, I. Mitchell, I. Rouse, M. Rudnicki, K. Sayanagi, H. Sloan and L. Parson, Direct evidence for the distribution and occurrence of hydrothermal activity between 27°N–30°N on the Mid-Atlantic Ridge, Earth Planet. Sci. Lett. 125, 119–128, 1994.

[8] H.D. Needham, O. Dauteuil, R. Detrick and C. Langmuir, Structural and volcanic features of the Mid-Atlantic Ridge rift zone between 40°N and 33°N, EOS, Trans. Am. Geophys. Union 43, 552, 1992.

[9] R.S. Detrick, H.D. Needham and V. Renard, Gravity anomalies and crustal thickness variations along the Mid-Atlantic Ridge between 33°N and 40°N, J. Geophys. Res. 100, 3767–3787, 1995.

[10] H. Sloan and P. Patriat, Kinematics of the North American–African plate boundary between 28° and 29°N during 10 Ma: evolution of the axial geometry and spreading rate and direction, Earth Planet. Sci. Lett. 113, 323–341, 1992.
[11] G. Klinkhammer, C. Chin and C. Wilson, Surveys of the FARA section of Mid-Atlantic Ridge for Hydrothermal activity during FAZAR, EOS, Trans. Am. Geophys. Union 74, 380, 1993.
[12] J.L. Charlou, H. Bougault, J.P. Donval, H. Pellé, C. Langmuir and the FAZAR Scientific Party. Seawater CH_4 concentration over the Mid-Atlantic Ridge from the Hayes F.Z. to the Azores Triple Junction, EOS, Trans. Am. Geophys. Union 74, 380, 1993.
[13] G.P. Klinkhammer, C.S. Chin. C. Wilson and C.R. German, Venting from the Mid-Atlantic Ridge at 37°17′N: The Lucky Strike Hydrothermal Site, in: Hydrothermal Vents and Processes, L.M. Parson, C.L. Walker and D.R. Dixon, eds., Geol. Soc. London Spec. Publ. 87, 87–96, 1995.
[14] C.H. Langmuir, D. Fornari, D. Colodner, J.L. Charlou, I. Costa, D. Desbruyeres, D. Desonie, T. Emerson, A. Fiala-Medioni, Y. Fouquet, S. Humphris, L. Saldanha, R. Sours-Page, M. Thatcher, M. Tivey, C. Van Dover, K. Von Damm, K. Wiese and C. Wilson, Geological setting and characteristics of the Lucky Strike vent-field at 37°17′N on the Mid-Atlantic Ridge, EOS, Trans. Am. Geophys. Union 74, 99, 1993.
[15] Y. Fouquet, J.L. Charlou, J.P. Donval, J. Radford-Knoery, H. Pellé, H. Ondréas, M. Ségonzac, I. Costa, N. Lourenço and M.K. Tivey, Geological setting and comparison of the Menez Gwen and Lucky Strike vent fields at 37°17′N and 37°50′N on the Mid Atlantic Ridge. Preliminary results of the DIVA1 diving cruise with Nautile, EOS, Trans. Am. Geophys. Union 75, 313, 1994.
[16] M.D. Rudnicki, R.H. James and H. Elderfield, Near-field variability of the TAG non-buoyant plume, 26°N, Mid-Atlantic Ridge, Earth Planet. Sci. Lett. 127, 1–10, 1994.
[17] C.S. Chin, G. Klinkhammer, C. Wilson, M. Rudnicki, C. German, B. Murton, H. Elderfield and R. James, Distribution and characteristics of hydrothermal plumes over the Mid-Atlantic Ridge. EOS, Trans. Am. Geophys. Union 75, 308, 1994.
[18] E.T. Baker and S.R. Hammond, Hydrothermal venting and the apparent magmatic budget of the Juan de Fuca Ridge, J. Geophys. Res. 97, 3443–3456, 1992.
[19] C.R. German, E.T. Baker and G. Klinkhammer, The regional setting of hydrothermal vents, in: Hydrothermal Vents and Processes, L.M. Parson, C.L. Walker and D.R. Dixon, eds., Geol. Soc. London Spec. Publ. 87, 3–15, 1995.
[20] C.R. German, J. Briem, C. Chin, M. Danielsen, S. Holland, R. James, A. Jónsdottir, E. Ludford, C. Moser, J. Ólafsson, M.R. Palmer and M.D. Rudnicki, Hydrothermal activity on the Reykjanes Ridge: the Steinahóll vent-field at 63°06′N, Earth Planet. Sci. Lett. 121, 647–654, 1994.
[21] R.S. Detrick, J. Honnorez and Leg 106 Scientific Party, Drilling the Snake Pit hydrothermal field on the Mid Atlantic Ridge, Lat. 23°22′N, Geology 14, 1004–1007, 1986.
[22] R.D. Ballard, J. Francheteau, T. Juteau, C. Rangan and W. Normark, East Pacific Rise at 21°N: the volcanic, tectonic and hydrothermal processes at the central axis, Earth Planet. Sci. Lett. 55, 1–10, 1981.
[23] R.M. Haymon, D.J. Fornari, K.L. Von Damm, M.D. Lilley, M.R. Perfit, J.M. Edmond, W.C. Shanks III, R.A. Lutz, J.M. Grebmeier, S. Carbotte, D. Wright, E. McLaughlin, M. Smith, N. Beedle and E. Olson, Volcanic eruption of the mid-ocean ridge along the East Pacific Rise crest at 9°45–52′N: Direct submersible observations of seafloor phenomena associated with an eruption event in April, 1991, Earth Planet. Sci. Lett. 119, 85–101, 1993.
[24] R.M. Haymon, D.J. Fornari, M. Edwards, S.M. Carbotte, D. Wright and K.C. McDonald, Hydrothermal vent distribution along the East Pacific Rise crest (9°09′–54′N) and its relationship to magmatic and tectonic processes on fast spreading mid-ocean ridges, Earth Planet. Sci. Lett. 104, 513–534, 1991.
[25] D.J. Wright, R.M. Haymon and D.J. Fornari, Crustal fissuring and its relationship to magmatic and hydrothermal processes on the East Pacific Rise crest (9°12′ to 54′N), J. Geophys. Res. 100, in press.